論文 한국정밀공학회지 제10권 제4호 1993.12
Journal of the Korean Society of Precision Engineering Vol. 10. No.4 Dec. 1993.

퓨리에 변환 격자법을 이용한 스트레인 속도 분포의 해석

양 인 홍*

Analysis of Strain Rate Distribution using Fourier Transform Grid Method

In-Hong Yang*

ABSTRACT

고속으로 변형을 받는 재료의 변형 강도는 정적인 부하를 받는 경우와는 다르며 이 고속 현상을 해석하기 위해서는 시간적, 공간적 변화를 조사할 필요가 있다. 일반적으로 스트레인 속도를 구하는 데는 스트레인 게이지를 이용하고 있지만, 고무와 같은 대변형을 하는 물체에서는 정확한 데이터를 얻기가 곤란하므로 스플라인 함수를 이용해서 보간 작업을 해야 한다. 그래서, 최근에는 스트레인 속도를 구하는 방법으로 격자법, 모아레법, 광탄성법 등이 이용되고 있다. 재료의 변위 분포를 구하는 데는 격자법이 잘 이용되어지고 있지만 스트레인 속도 분포의 해석의 정도에 문제가 되고 있다. 이러한 문제를 해결하기 위하여 본 논문에서는, 고속으로 변형하는 물체의 형상을 역학적으로 해석하기 위해 고속도 카메라로 촬영을 하고 그 때 얻어진 격자 화상을 퓨리에 변환 격자법을 이용해서 위상을 구하고 스트레인 속도 분포를 해석했다.

Key Words : Fourier Transform Grid Method, Strain Rate, Image Processing, Fringe Analysis

1. INTRODUCTION

Strain rates are especially important because the behavior of materials under shock loading is different from that under static loading. It is necessary to know the mechanical properties of the materials involved at the strain rates to which the structural components are subjected. In order to measure displacement distributions of materials under large deformation, the Fourier transform grid method using the first harmonic of the Fourier spectrum of the deformed grid images is useful. Parks[1] has presented a method of analysis of strain using grid. Scimmarella and Sturgeon[2] have developed a method for analyzing the phases of mismatched fringes by using the one-dimensional Fourier transform. Moreover, Takeda and Mutoh[3] have developed the Fourier transform profilometry. In this method, the shape of an object can be measured by calculating the phases of the Fourier spectrum of the grating projected on the object. Yang and Morimoto et al[4-6]. have previously developed the Fourier transform grid method for analyzing a fringe pattern recorded by an image processor. In this method, the first harmonic

* 제주대학교 해양환경공학과(정회원)

of the intensity distribution of a grid or fringe pattern is extracted to obtain the phase distribution. This phase analysis provides more accurate analysis than the conventional method.

For experimental observations of the behavior of materials under high rates of deformation, a high speed video camera is useful. There are two types of solid-state image sensors : the CCD type and the MOS type. Although the CCD type is popular for an ordinary video camera, it is difficult to make the frame speed faster. Solid-state image sensors are excellent from the view point of dimensional accuracy and stabilty. The frame speed becomes faster when a small scanning area is selected. High speed frame recording was performed by dividing the scanning area of the image sensor, while the Fourier transform grid method was extended to obtain strain rate distribution. In this paper, the images recorded by the high speed video camera with the MOS type of image sensor are analyzed by the Fourier transform grid method. Both the strain distribution and the strain rate distribution are analyzed by differentiating displacement with respect to distance and time. Since the analysis of strain rate requires differentiation of displacement data, it is difficult to obtain good accuracy by conventional methods. Using the Fourier transform grid method, smoothing of data is naturally performed and sufficiently meaningful results are obtained. As an example, the stress wave propagation in a rectangular rubber plate is recorded by the high speed video camera, and the strain rate distribution is analyzed by the extended Fourier tansform grid method.

2. THEORY OF ANALYSIS

Figure 1 shows rectangular brightness intensity distribution of a model grating before deformation. The grating has a rectangular brightness distribution consisting of alternate dark and bright stripes whose brightnesses are zero and E, respectively. The expansion of the grating intensity function, f(x), in Fourier series is

$$f(x) = \sum_{n=-\infty}^{+\infty} C_n \exp \{ j2\pi n\omega_o (x - x_o) \}, \quad (1)$$

where

$$C_n = C_o \sin (\pi n b_o / P_o) / (\pi n b_o / P_o) \quad (2)$$

$$C_o = E b_o / P_o. \quad (3)$$

and j is the imaginary unit, n is an integer. The initial spatial frequency ω_o of the grating is defined as

$$\omega_o = 1 / P_o. \quad (4)$$

where P_o is the grating pitch, b_o is the width of the bright part of the grating. The ratio α of the bright line width b_o to the pitch P_o,

$$\alpha = b_o / P_o. \quad (5)$$

is called the opening ratio of the grating and is a specific property of the grating together with the grating pitch.

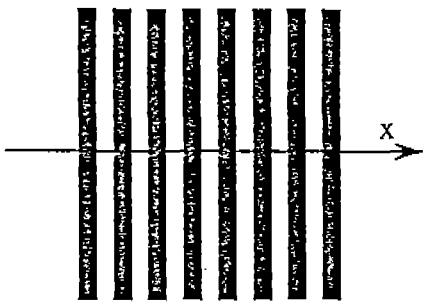

(a) Grating pattern

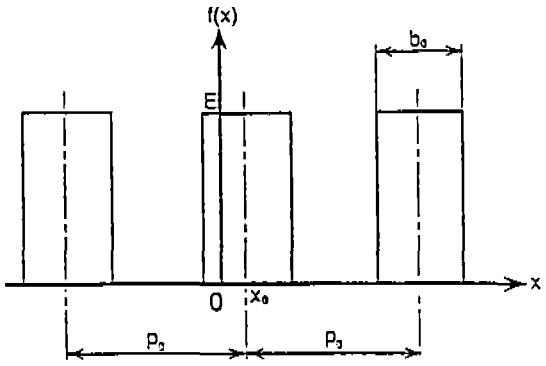

(b) Brighteness intensity distribution

Fig. 1 Brightness distribution of a model grating before deformation

If the displacement at any point X and at any time t is u(X, t), the relationship between point X during the deformation at time t and the initial position x of the same point before deformation is expressed as

$$X = x + u(X, t). \tag{6}$$

The grating intensity function g(X, t) at a point X during deformation corresponds to the grating intensity f(x) in the initial position x. Thus,

$$\begin{aligned} g(X, t) &= f(x) \\ &= f\{X - u(X, t)\} \\ &= \sum_{n=-\infty}^{\infty} C_n \exp\{j2\pi n\omega_0 (X - u(X, t))\} \\ &= \sum_{n=-\infty}^{\infty} i_n(X, t)\exp(j2\pi n\omega_0 X) \end{aligned} \tag{7}$$

where $i_n(X, t)$ is

$$i_n(X, t) = C_n \exp[-j2\pi n\omega_0\{u(X, t) + x_0\}]. \tag{8}$$

The computation of the Fourier transform of the grating pattern expressed in Eq. (7) gives

$$\begin{aligned} G(\Omega, t) &= \int_{-\infty}^{\infty} g(X, t) \exp(-j2\pi \Omega X)dX \\ &= \sum_{n=-\infty}^{\infty} I_n(\Omega - n\omega_0, t). \end{aligned} \tag{9}$$

where $I_n(\Omega - n\omega_0, t)$ is defined as the Fourier transform of the function $i_n(x, t)$. Figure 2 schematically illustrates the spectra obtained by the transform. Each spectrum corresponds to the nth harmonic. Now, from Fig. 2 the first harmonic $I_1(\Omega - n\omega_0, t)$ is extracted from these spectra using a band-pass filter as indicated by the oblique lines. Computing the inverse Fourier transform of $I_1(\Omega - n\omega_0, t)$,

$$i_1(X, t) = \int_{-\infty}^{\infty} I_1(\Omega - \omega_0, t) \exp(j2\pi \Omega X)d\Omega \tag{10}$$

is obtained. By the variable transforming $\alpha = \Omega - \omega_0$,

$$i_1(X, t) = C_1 \exp[j2\pi\omega_0\{X - u(X, t) - x_0\}] \tag{11}$$

is obtained. This grating was reconstructed from only the first harmonic of Eq. (7). That is, the grating with a rectangular brightness distribution is reconstructed as a grating with a sinusoidal

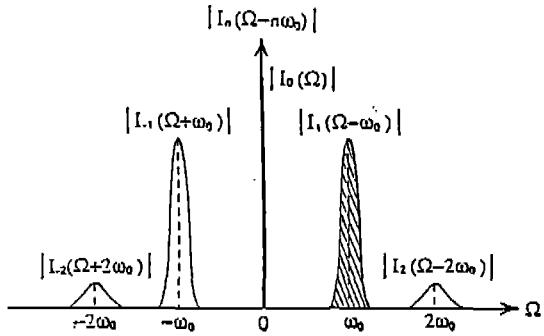

Fig. 2 Fourier spectra of model grating

brightness distribution excluding the higher harmonic by filtering.

The argument of Eq. (11) or the phase of the fringe is expressed as

$$\theta(X, t) = 2\pi\omega_0\{X - u(X, t) - x_0\} \tag{12}$$

which includes the displacement u(X, t). Calculating the arctangent of the ratio of the imaginary part to the real part of the complex pattern, we compute the argument as follow :

$$\theta(X, t) = \tan^{-1}\left[\frac{\mathrm{Im}\{i_1(X, t)\}}{\mathrm{Re}\{i_1(X, t)\}}\right]. \tag{13}$$

The displacement u(X, t) is obtained by Eq. (12) after calculating the argument θ(X, t) in Eq. (13) from the complex grating pattern.

The Eulerian strain ε^E and displacement velocity u^E are obtained from the displacement as follws :

$$\varepsilon^E(X, t) = \frac{\partial u(X, t)}{\partial X}, \tag{14}$$

$$\dot{u}^E(X, t) = \frac{\partial u(X, t)}{\partial t}. \tag{15}$$

The displacement velocity obtained by Eq. (15) is the velocity on the Eulerian view which is obtained by differentiating the displacement in fixed space with respect to time. In solid mechanics, the displacement velocity on the Lagrangian view, which is obtained by differentiating the displacement in material space, is imporant. In the remainder of this paper, velocity and strain rate indicate those on the Lagrangian view unless otherwise mentioned.

The grating treated in this paper has continuous displacement with respect to position and time. The conversion equation from the Eulerian variable to Lagrangian one is given as

$$\left(\frac{\partial u}{\partial t}\right)_x = \left(\frac{\partial u}{\partial t}\right)_X + \frac{\partial u}{\partial X}\left(\frac{\partial u}{\partial t}\right)_x, \tag{16}$$

where the suffix x is with respect to the Lagrangian variable and suffix X is with respect to the Eulerian variable. When the velocity in Lagrangian coordinates is denoted as $u^L(X, t)$, the values in Eq. (16) become

$$\left(\frac{\partial u}{\partial t}\right)_x = \dot{u}^L(X, t), \quad \left(\frac{\partial u}{\partial t}\right)_X = \dot{u}^E(X, t),$$
$$\frac{\partial u}{\partial X} = \varepsilon^E(X, t), \quad \left(\frac{\partial u}{\partial t}\right)_x = \dot{u}^L(X, t). \tag{17}$$

Therefore, using Eqs. (16) and (17), the velocity in Lagrangian coordinates is claculated by

$$\dot{u}^L(X, t) = \dot{u}^E(X, t)/\{1 - \varepsilon^E(X, t)\}. \tag{18}$$

From the velocity, the strain rate in Lagrangian coordinates is calculated by

$$\dot{\varepsilon}^E(X, t) = \partial\dot{u}^L(X, t)/\partial X. \tag{19}$$

3. APPLICATIION TO A RECTANGULAR RUBBER PLATE

Stress wave propagation in a rectangular rubber plate is obtained by analyzing grating images recorded by a high speed video camera. The digital image taken by the high speed video camera is analyzed by an image processing system using a personal computer. The frame speed or image size of this video camera and the solid-state image sensor, HE98246, made by Hitachi Ltd, are controlled by a personal computer. We are considering a system in which the blanking period is eliminated by passing the NTSC system and directly recording the image using an A/D converter and digital image memories. Of course, it is possible to directly

connect the high speed video camera to the image memory. The recorded image is analyzed by the methods mentioned above using the personal computer. Since the image sensor can be operated using twice the frequency of the current clock, the video camera will operate at a speed of more than 10 million frames/s. The output image signal is recored on a video tape recorder. The analog signal of the images on the video tape recorder is converted to digital images in the image memory by an A/D converter and stored in the frame memory of the image grabber. If the image signal is sent to the same IC memories by cyclically rewriting, the desired images are stored by sending a trigger after the phenomenon is completed.

In order to analyze strain rate distribution of a rectangular rubber plate, the measurement system shown in Fig. 3 is used. The specimen is a rectangular rubber plate whose size is 450 × 20 × 10mm. A one-dimensional grating pattern with a plate 8mm is drawn on the rubber plate. The grating image before deformation recorded by a high speed video camera is shown in Fig. 4. The rubber plate is stretched in the vertical direction, and the grating pitch after stretching is 8.67mm. The camera position is adjusted to coincide to a pitch with a 17 pixels length of image memory. After the upper of the rubber plate is cut, an unloading stress wave propagates and the rubber plate shrinks after propagation. The images are analyzed by the Fourier transform using the personal computer. The image size is 512 pixels in the horizontal direction and 200 pixels in the vertical direction. This deformation is considered to be one-dimensional so that the two vertical pixels are separated into two different time data. Thus, the frame rate in this case corresponds to 15730 frames/s. Because the camera is rotated 90 degrees, the left side of the image corresponds to the upper section of the rubber

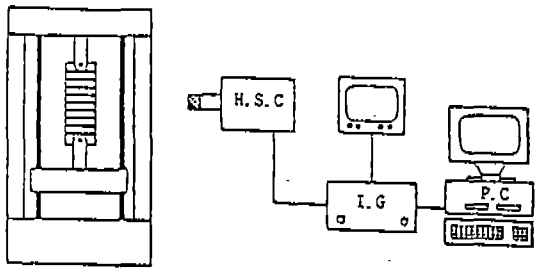

Fig. 3 Measurement system

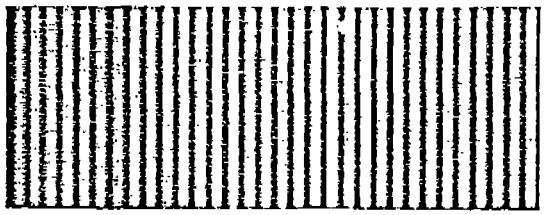

Fig. 4 Grating image before deformation by high speed camera

plate.

Fig. 5 shows the grating lines moving from the left to the right when an unloading wave is propagating. The direction is computed on each time line Fig. 6 shows the Fourier power spectra of Fig. 5. In this figure, the downward direction shows the time coordinate, and the horizontal direction shows the frequency. The origin of the frequency is the vertical line at the center of the figure. The right domain from the center is the positive frequency in proportion to the distance from the origin, and the left domain from the center is the negative frequency. The brightness intensity of this figure corresponds to the power intensity of the frequency. Fig. 7 shows the first harmomic extracted from the right side region, 27 to 53 pixels away from the origin of Fig. 6. Fug. 8 shows the displacement distribution obtained by calculating the phases of the first harmonic. By differentiating the displacement with respect to distance using Eq. (14) and substituting it into

Eq. (18), strain distribution is obtained, as shown in Fig. 9. The velocity distribution obtained by differentiating the displacement with respect to time using Eq. (15) and substituting it into Eq. (18) as shown in Fig. 10. The differentiation of the velocity using Eq. (19) gives the strain rate distribution shown in Fig. 11. The inclination of the wavefront in Fig. 11 shows the propagation velocity of the stress wave. In this case, the velocity is 57.5 m/s. The wavefront with a high strain rate is clearly observed.

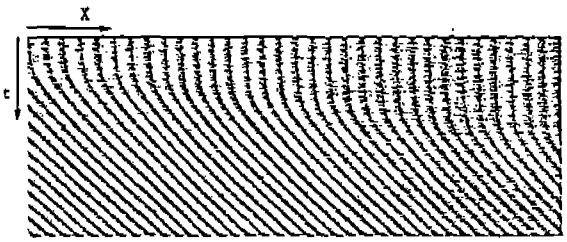

Fig. 5 Grating image under deformation by high speed camera

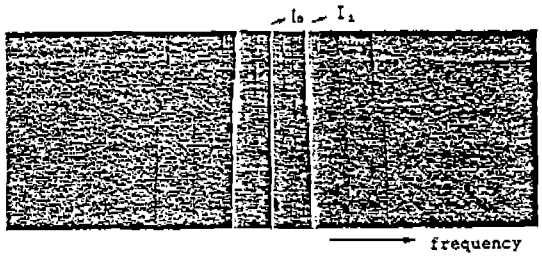

Fig. 6 Fourier spectra of Fig. 5

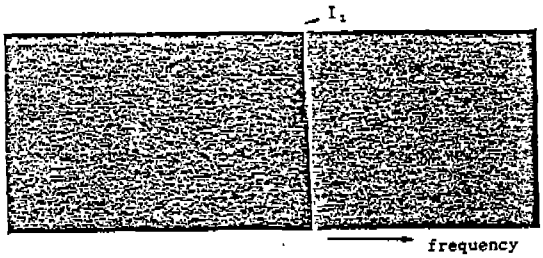

Fig. 7 Extracted first harmonic

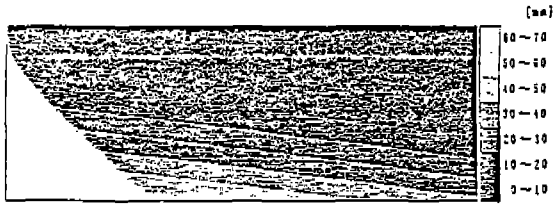

Fig. 8 Displacement distribution

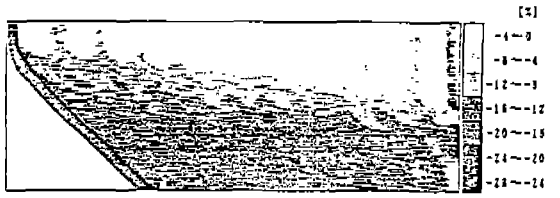

Fig. 9 Strain distribution

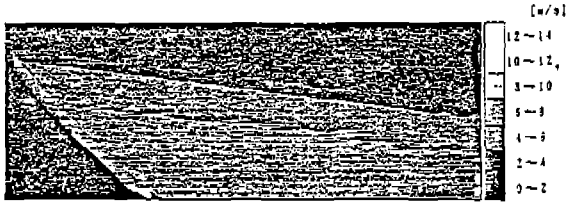

Fig. 10 Velocity distribution

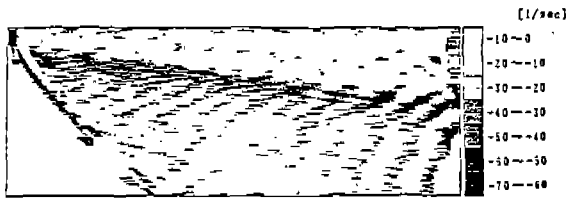

Fig. 11 Strain rate distribution

4. CONCLUSIONS

By improving the Fourier transform grid method, the strain rate distribution in a rectangular rubber plate is measured. The recorded image taken by the high speed video camera is analyzed by the Fourier transform grid method mentioned above. Using the Fourier transform grid method and the high speed video camera, stress wave propagation in a

rectangular rubber plate has been analyzed to obtain the distributions of displacement, strain, velocity and strain rate. The new Fourier transform grid method is eliminated high-frequency noise, so that meaningful results were obtained.

REFERENCES

1. V. J, Parks, "Strain measurement using grids", Optical Engineering, Vol. 21, No. 4, pp. 663~639, 1982.
2. C. A. Scimmarella and D. L. Sturgeon, "Digital-filtering Techincques Applied to the Interpolating of Moire-fringes Data", Exep. Mech., Vol. 7, No. 11, pp. 468~475, 1967.
3. M. Takeda and K. Mutoh, "Fourier Transform Profilometry for Automatic Measurement of 3D Object Shapes", Appl. Opt., Vol. 22, No. 24, pp. 3977~3982, 1984.
4. I. H. Yang, M. Fujigaki, Y. Morimoto and E. K. Han, "Strain Analysis of Vibrating Object using Fourier Transform Grid Method", Journal of JSNDI(in Japanese), Vol. 41, No. 8, pp. 486~492, 1992.
5. Y. Morimoto, "Image Processing Aided Analysis of Stress, Strain, Deformation and Shape", JSME, Vol. 55, No. 11, pp. 365~372, 1988.
6. I. H. Yang, "Strain Analysis using Fourier Transform Grid Method and Its Image processing", Journal of the Korean Society of Precision Engineering, Vol. 9, No. 3, pp. 165~171, 1992.